



## The interactions between olivine dissolution and phytoplankton in seawater: Potential implications for ocean alkalinization

Canru Li<sup>a</sup>, Xiangdong Liu<sup>b</sup>, Yan Li<sup>a</sup>, Yuan Jiang<sup>b</sup>, Xianghui Guo<sup>a</sup>, David A. Hutchins<sup>c</sup>, Jian Ma<sup>d</sup>, Xin Lin<sup>a,\*</sup>, Minhan Dai<sup>a</sup>

<sup>a</sup> State Key Laboratory of Marine Environmental Science, College of Ocean and Earth Sciences, Xiamen University, Xiamen 361102, PR China

<sup>b</sup> College of Materials, Higher Educational Key Laboratory for Biomedical Engineering of Fujian Province, Fujian Key Laboratory of Advanced Materials, Xiamen University, Xiamen 361005, PR China

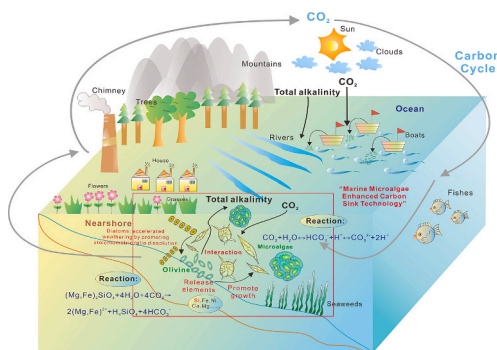
<sup>c</sup> University of Southern California, Los Angeles, CA, USA

<sup>d</sup> State Key Laboratory of Marine Environmental Science, College of the Environment and Ecology, Xiamen University, Xiamen 361102, PR China

### HIGHLIGHTS

- Olivine dissolution promotes the growth of phytoplankton.
- The highly silicified diatom benefits most from olivine dissolution.
- Diatoms promote olivine dissolution by enhancing stoichiometric dissolution.

### GRAPHICAL ABSTRACT



### ARTICLE INFO

Editor: José Virgílio Cruz

#### Keywords:

Carbon dioxide removal  
Diatoms  
Microalgae  
Silicate mineral  
Stoichiometric dissolution  
Seawater

### ABSTRACT

Ocean alkalinity enhancement, one of the ocean-based CO<sub>2</sub> removal techniques, has the potential to assist us in achieving the goal of carbon neutrality. Olivine is considered the most promising mineral for ocean alkalinization enhancement due to its theoretically high CO<sub>2</sub> sequestration efficiency. Olivine dissolution has been predicted to alter marine phytoplankton communities, however, there is still a lack of experimental evidence. The olivine dissolution process in seawater can be influenced by a range of factors, including biotic factors, which have yet to be explored. In this study, we cultivated two diatoms and one coccolithophore with and without olivine particles to investigate their interactions with olivine dissolution. Our findings demonstrate that olivine dissolution promoted the growth of all phytoplankton species, with the highly silicified diatom *Thalassiosira pseudonana* benefiting the most. This was probably due to the highly silicified diatom having a higher silicate requirement and, therefore, growing more quickly when silicate was released during olivine dissolution. Based on the structural characteristics and chemical compositions on the exterior surface of olivine particles, *T. pseudonana* was found to promote olivine dissolution by inhibiting the formation of the amorphous SiO<sub>2</sub> layer on the surface of olivine and therefore enhancing the stoichiometric dissolution of olivine. However, the positive effects of

\* Corresponding author.

E-mail address: [xinlinulm@xmu.edu.cn](mailto:xinlinulm@xmu.edu.cn) (X. Lin).

<https://doi.org/10.1016/j.scitotenv.2023.168571>

Received 28 July 2023; Received in revised form 6 October 2023; Accepted 12 November 2023

Available online 17 November 2023

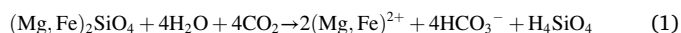
0048-9697/© 2023 Elsevier B.V. All rights reserved.

*T. pseudonana* on olivine dissolution were not observed in the coccolithophore *Gephyrocapsa oceanica* or the non-silicate obligate diatom *Phaeodactylum tricorutum*. This study provides the first experimental evidence of the interaction between phytoplankton and olivine dissolution, which has important implications for ocean alkalization research.

## 1. Introduction

Annual carbon dioxide (CO<sub>2</sub>) emissions have exceeded 40 Gt (Friedlingstein et al., 2022), significantly contributing to global warming. To keep warming well below 2 °C, annual 5 Gt CO<sub>2</sub> by 2050 should be removed from the atmosphere (IPCC, 2022; Rogelj et al., 2018). To meet this goal, negative emission technologies (NETs) must be deployed quickly and widely (Hilaire et al., 2019; Rockström et al., 2017). Among the proposed carbon dioxide removal (CDR) strategies (National Academies of Sciences E, Medicine, 2021; Pozo et al., 2020), ocean alkalinity enhancement involves the addition of alkaline substances to seawater to enhance the ocean's natural carbon sink and alleviate ocean acidification (González and Ilyina, 2016; Kheshgi, 1995). The silicate mineral olivine ((Mg, Fe)<sub>2</sub>SiO<sub>4</sub>) is considered a promising candidate mineral for ocean alkalization due to its high carbon sequestration per mole, long-term carbon sequestration, widespread availability, and high abiotic dissolution rate per unit surface area (Goll et al., 2021; Oelkers et al., 2018; Rigopoulos et al., 2018).

The chemical equation for olivine dissolution is:



Thus theoretically, 4 mol of protons are consumed for each mole of olivine dissolved, thus producing 4 mol of alkalinity, and absorbing 4 mol of CO<sub>2</sub> (Bach et al., 2019). The impacts of abiotic factors on olivine dissolution in fresh water and terrestrial systems, such as mineral types reactivity, grain sizes, temperature, salinity, CO<sub>2</sub> pressure and pH have been widely studied (Hangx and Spiers, 2009; Prigione et al., 2009; West et al., 2005). Biological activity can greatly accelerate the weathering of olivine and the uptake of CO<sub>2</sub> (Schuiling and Boer, 2011). Both positive and negative effects of microorganisms such as fungi and bacteria on the dissolution or weathering of other minerals have been reported (Gerrits et al., 2020; Jongmans et al., 1997; Oelkers et al., 2015; Seiffert et al., 2014; Shirokova et al., 2012; Vicca et al., 2022).

However, a few studies focusing on olivine dissolution in seawater have been reported. Montserrat et al. (2017) reported that olivine dissolution in artificial and natural seawater caused a significant increase in alkalinity and dissolved inorganic carbon (DIC) due to CO<sub>2</sub> sequestration. It has been predicted that dissolved ions such as bicarbonate, silicic acid, and iron released from olivine dissolution, may promote the growth of phytoplankton, particularly diatoms, leading to enhanced carbon capture capacity and a shift in phytoplankton species composition in the ocean (Bach et al., 2019; Hutchins et al., 2023). The nickel, cobalt, and chromium released from olivine dissolution are potentially toxic to marine organisms. However, laboratory or field studies of the effects of olivine dissolution on phytoplankton are still severely lacking. Although freshwater microalgae have been shown to enhance the olivine dissolution rate (Xie and Wu, 2014; Xie et al., 2023). It is still an open question whether marine phytoplankton can promote olivine dissolution in seawater.

In this study, we cultivated three phytoplankton species, including two diatoms and one coccolithophore, with and without olivine particles to investigate the interactions between phytoplankton and olivine dissolution. Time-resolved chemical parameters in seawater and physiological parameters of phytoplankton were measured. We further examined the chemical compositions and structural characteristics on the exterior surface of the olivine in biotic and abiotic conditions. Here, we would like to address the following questions: (1) Whether olivine dissolution can promote the growth of phytoplankton in seawater; (2) Whether diatoms benefit more from olivine dissolution in seawater. To

our best knowledge, this is the first experimental-based study on the interactions between phytoplankton and olivine dissolution in seawater, which aims to help us better understand the underlying mechanisms of olivine dissolution in seawater from a multidisciplinary perspective.

## 2. Material and methods

### 2.1. Composition and particle characteristics of olivine particles

Natural olivine particles (1–3 mm diameter) were purchased from 3A Materials (CAS: 15118-03-3) and were grinded up using a QM-3SP2 planetary ball mill. Olivine particles (particle size quantiles: D10 = 1.520 μm, D50 = 6.135 μm, D90 = 22.439 μm) had a molar Fe-to-Mg ratio of 0.08:0.92, characterizing the olivine as forsterite-92 (Fo92). The details of composition and particle characteristics of olivine particles are in Text S1, Table S1 and Table S2.

### 2.2. Strains and culture conditions

The coccolithophore *Gephyrocapsa oceanica* (G. o), the highly silicified diatom *Thalassiosira pseudonana* (T. p) and the non-silicate obligate diatom *Phaeodactylum tricorutum* (P. t) were used in this study (Text S2). These phytoplankton were cultured in 1 L polycarbonate bottles filled with 1 L of artificial seawater (Table S3) at an initial cell concentration of 2 × 10<sup>4</sup> cells mL<sup>-1</sup>, then 0.1 g olivine particles was added to 1 L of phytoplankton culture. Culture conditions are shown in Text S2.

### 2.3. Chl *a* and PSII photochemical efficiency measurement

The chlorophyll *a* (Chl *a*) concentration was calculated by the following equations: Chl *a* (μg mL<sup>-1</sup>) = 13.2654 × (A<sub>665</sub> - A<sub>750</sub>) - 2.6839 × (A<sub>632</sub> - A<sub>750</sub>) (Strickland and Parsons, 1972). The maximum Chl *a* concentration was calculated based on the fitted logistic equation. PSII photochemical efficiency (Φ<sub>PSII</sub>) was determined by a hand-held algal fluorometer (AquaPen AP110/C) (Genty et al., 1989). Details are in Text S3.

### 2.4. Carbonate system parameters and silicate concentration measurement

An AS-ALK2 TA titrator was used to measure the amount of total alkalinity (TA) in the samples (APOLLO SCITECH, USA). An AS-C3 total DIC analyzer was used to determine the amount of total dissolved inorganic carbon (DIC) in the samples (APOLLO SCITECH, USA). Details are in Text S4. An automatic nutrient analyzer (AA3, SEAL, Germany) was used to determine the Si(OH)<sub>4</sub> concentrations of samples. Details are in Text S5.

### 2.5. Olivine surface characterization

We used Zeiss HD scanning electron microscopy (SEM) equipped with energy dispersive spectroscopy (EDS) and X-ray photoelectron spectroscopy (XPS) to analyze the structural characteristics and chemical compositions on the exterior surface of olivine particles in biotic and abiotic conditions. Details are in Text S6.

### 3. Results and discussion

#### 3.1. Olivine dissolution can promote the growth of phytoplankton in seawater

No significant difference in Chl *a* concentration was detected between *G. oceanica* cultures with and without olivine addition (Fig. 1a). At hours 144 and 192, the Chl *a* concentration in *T. pseudonana* culture with olivine was significantly higher than in cultures without olivine (Fig. 1b). At hours 144 and 312, *P. tricorutum* cultured with olivine had a significantly higher Chl *a* level (Fig. 1c), but the difference was not as pronounced as it was in *T. pseudonana*. No significant difference in  $\Phi_{\text{PSII}}$  was detected between *G. oceanica* cultures with and without olivine addition (Fig. 1d). At hours 144, 168, and 192, the  $\Phi_{\text{PSII}}$  in *T. pseudonana* culture with olivine was significantly higher than in cultures without olivine (Fig. 1e). At hour 144, the  $\Phi_{\text{PSII}}$  in *P. tricorutum* culture with olivine was significantly higher than in cultures without olivine (Fig. 1f), however, the difference was not as pronounced as it was in *T. pseudonana*. Our findings suggest that diatoms benefited significantly from olivine dissolution in terms of photosynthetic efficiency. The calculated maximum Chl *a* concentration based on the fitted logistic equation was higher in the culture with olivine than without olivine in three species of phytoplankton. The promotion of phytoplankton growth by olivine varied: *T. pseudonana* > *P. tricorutum* > *G. oceanica* (Table S4). The maximum Chl *a* concentration based on the fitted logistic equation of *G. oceanica* culture with and without olivine addition was  $453 \mu\text{g L}^{-1}$  and  $325 \mu\text{g L}^{-1}$ , respectively, with the culture with olivine addition having 1.39 times higher Chl *a* concentration. The maximum Chl *a* concentrations of *T. pseudonana* with and without olivine addition were  $477 \mu\text{g L}^{-1}$  and  $201 \mu\text{g L}^{-1}$ , respectively, with the Chl *a* concentrations being 2.37 times higher in the culture with olivine addition. For *P. tricorutum*, the maximum Chl *a* concentration of cultures with and without olivine was  $7070 \mu\text{g L}^{-1}$  and  $4508 \mu\text{g L}^{-1}$ , respectively, with 1.56 times Chl *a* concentration in the culture with olivine addition.

Our results demonstrate that olivine dissolution promoted the growth of phytoplankton and benefited diatoms more, especially *T. pseudonana* with its highly silicified frustule, which is consistent with a recent study (Hutchins et al., 2023). Our results showed that olivine dissolution favored diatoms the most while having little influence on coccolithophores. Therefore, we speculate that the biomass of diatoms will increase and phytoplankton composition will be altered if we use olivine for ocean alkalinity enhancement. Our findings are not entirely consistent with the modeling results, which indicated that coccolithophores will be losers while diatoms will be winners if the olivine dissolves in large quantities in the ocean (Bach et al., 2019). The neutral and positive effects of olivine dissolution on the growth of cyanobacteria were revealed by (Hutchins et al., 2023) using a synthetic olivine leachate (OL). It is worth noting that the impacts on phytoplankton based on the OL may differ from the effects of the olivine dissolution due to the low dissolution rate of olivine and the mineralization process during the olivine dissolution. As far as we know, the effects of olivine dissolution on dinoflagellates were not evaluated, which is worth further exploring. To better understand the potential ecological implications of olivine dissolution, additional studies on the effects of olivine dissolution on marine phytoplankton is necessary.

#### 3.2. The effects of olivine dissolution and phytoplankton's growth on carbonate system

In the artificial seawater with the presence of olivine and the absence of phytoplankton, the DIC concentration increased nearly linearly during the experiment, whereas the TA concentration increased dramatically from the beginning to hours 48 and then increased slightly to the end of the experiment (Fig. 2a). This could be a result of the olivine surface initially having more active sites for the reaction, but as dissolution continued and secondary phases were generated, the active surface area diminished, resulting in a slower dissolution rate (Oelkers et al., 2018). In general, the dynamics of carbonate parameters in phytoplankton cultures with or without olivine were mainly driven by

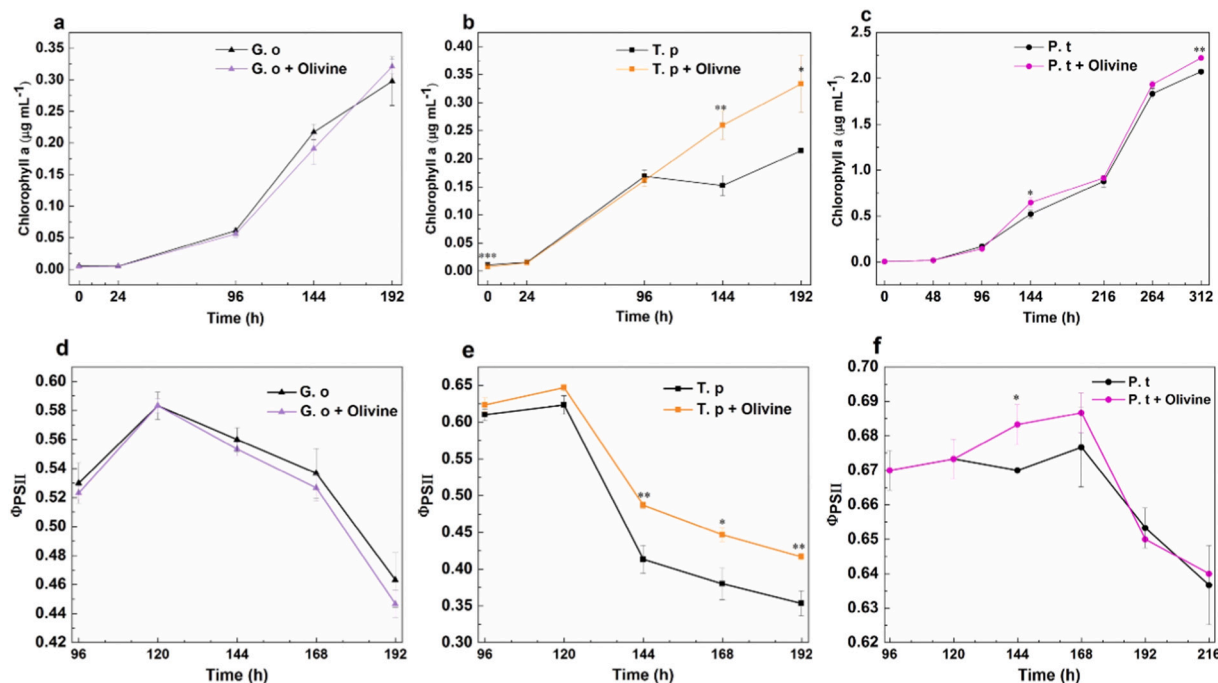
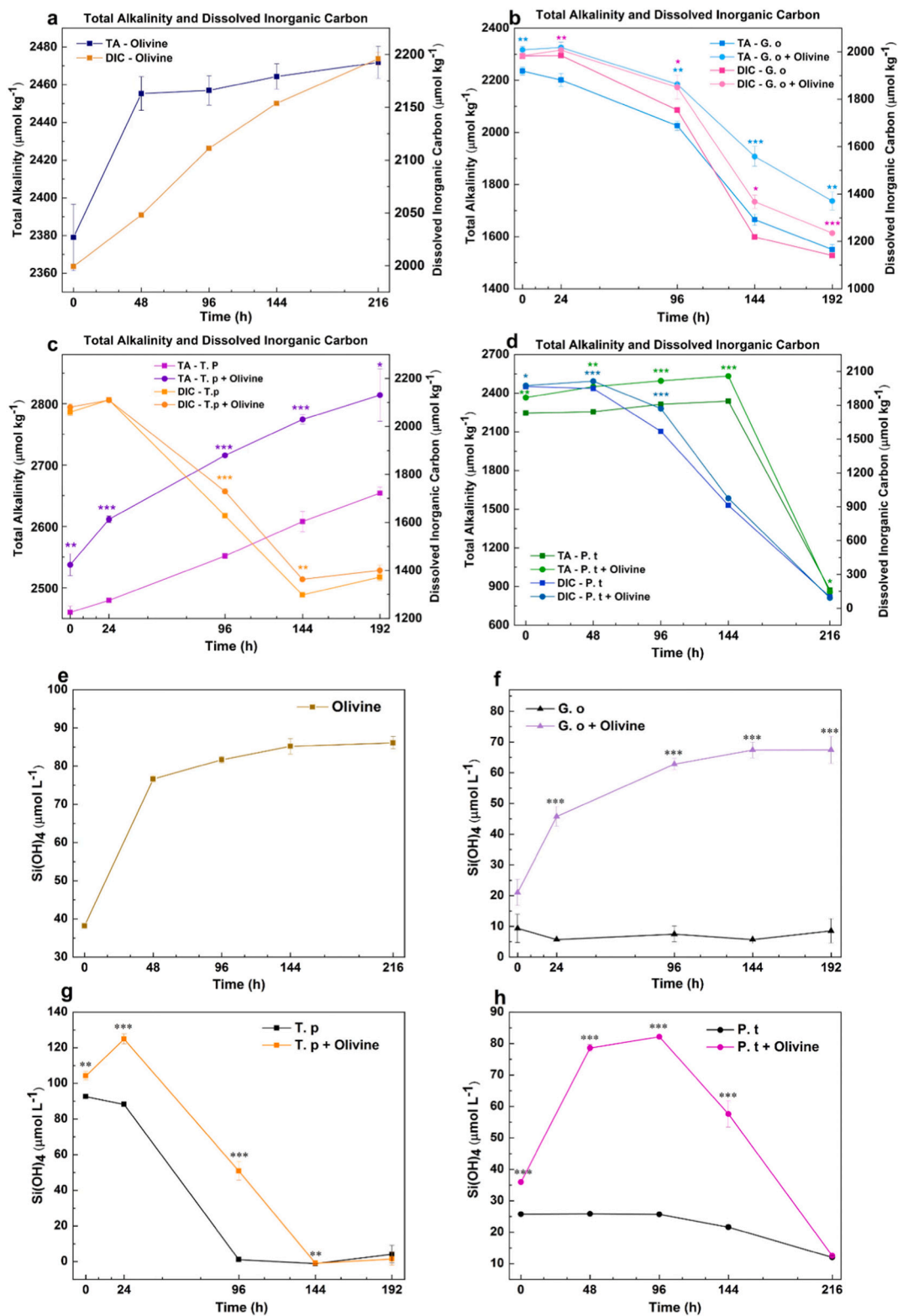


Fig. 1. The chlorophyll *a* concentration of *Gephyrocapsa oceanica* (*G. o*) (a), *Thalassiosira pseudonana* (*T. p*) (b), and *Phaeodactylum tricorutum* (*P. t*) (c) with or without olivine during the cultivation. The PSII photochemical efficiency ( $\Phi_{\text{PSII}}$ ) of *G. oceanica* (*G. o*) (d), *T. pseudonana* (*T. p*) (e), and *P. tricorutum* (*P. t*) (f) with or without olivine during the cultivation. Data are presented as the mean  $\pm$  SD ( $n = 3$ ). Significant changes between treatments are shown as symbols (\* $P < 0.05$ ; \*\* $P < 0.01$ ; \*\*\* $P < 0.001$ ).



**Fig. 2.** Changes in total alkalinity (TA), dissolved inorganic carbon (DIC), and Si(OH)<sub>4</sub> concentrations during the culture of three phytoplankton species with and without olivine addition. The changes in TA and DIC concentrations in artificial seawater medium without olivine (a), and cultures grown with or without olivine of *G. oceanica* (b), *T. pseudonana* (c) and *P. tricornutum* (d). The changes in Si(OH)<sub>4</sub> concentrations in artificial seawater with olivine (e), and in cultures grown with and without olivine of *G. oceanica* (f), *T. pseudonana* (g) and *P. tricornutum* (h). Data are presented as the mean  $\pm$  SD (n = 3). Significant changes between treatments are shown as symbols (\* $P < 0.05$ ; \*\* $P < 0.01$ ; \*\*\* $P < 0.001$ ).

the growth of phytoplankton. The TA declined during the cultivation of *G. oceanica* with or without olivine, which is consistent with a previous study showing that *G. oceanica* consumes 2 mols of TA to produce 1 mol of calcium carbonate, thereby lowering the TA (Fig. 2b) (Bach et al., 2019). TA values in *T. pseudonana* cultures with and without olivine addition both showed upward trend during cultivation (Fig. 2c). The photosynthetic activity of *T. pseudonana* needs protons drawn from their aquatic environment, which resulted in an increase in the culture medium's TA (Zerveas et al., 2021). The TA values in *P. tricornutum* cultures increased gradually but dropped abruptly to a very low level at the late stage of cultivation, probably due to very active bicarbonate absorption (Ouyang et al., 2018) by *P. tricornutum* (Fig. 2d). DIC concentrations in *G. oceanica*, *T. pseudonana*, and *P. tricornutum* cultures showed an overall decreasing trend as the phytoplankton absorbed bicarbonate for photosynthetic carbon fixation (Figs. 2b-d). Collectively, the TA values and DIC concentrations were generally higher in the phytoplankton cultures with olivine than in the cultures without olivine at different time points during the cultivation due to the increase of  $\text{HCO}_3^-$  caused by olivine dissolution (Figs. 2b-d). It is worth noting that olivine dissolved quite quickly after being added to seawater during the first hours, causing the carbonate system to change during the sampling process at our first sample time point.

The strategies of DIC uptake from the external environment to cells are diverse, ranging from diffuse  $\text{CO}_2$  uptake to active transport of  $\text{HCO}_3^-$  and  $\text{CO}_2$ , and many organisms have external carbonic anhydrases (eCA) to facilitate  $\text{HCO}_3^-$  utilization (Colman et al., 2002; Tsuji et al., 2017). Although  $\text{CO}_2$  is considered the major carbon source for algae growth, most algae are able to actively uptake bicarbonate using bicarbonate transporters (Giordano et al., 2005). The increase of  $\text{HCO}_3^-$  concentration in the culture medium has been shown to promote the growth of phytoplankton (Gardner et al., 2012; Huang et al., 2023; White et al., 2013). In our study, the promotion of phytoplankton growth by olivine was also probably due to the increase in bicarbonate caused by olivine dissolution, which is worth further exploration.

### 3.3. The silicate released from olivine dissolution was absorbed by *T. pseudonana*

The olivine dissolution in the artificial seawater without phytoplankton led to a sharp increase in silicate concentration within 48 h and then a slight increase until the end of the experiment, indicating silicate was released during the olivine dissolution (Fig. 2e). A similar increasing pattern of silicate concentration during the cultivation of *G. oceanica* with olivine indicated that *G. oceanica* did not absorb the silicate released from olivine dissolution (Fig. 2f). In contrast, diatoms were able to utilize the silicate released from olivine dissolution. Diatoms have a distinctive siliceous frustule, which results in a major silicate requirement for diatoms, especially for highly silicified species. Within 96 h, the silicate concentration in the cultures of *T. pseudonana* with olivine addition was significantly higher than that of the culture without olivine. During the later stages of cultivation, the silicate concentration in *T. pseudonana* with and without olivine addition all returned to a very low level, demonstrating that the silicate was taken up by *T. pseudonana* (Fig. 2g). It is considered that *P. tricornutum* lacks an obligate requirement for silicate, and thus frustule formation is facultative (Armbrust, 2009). In our study, *P. tricornutum* showed remarkable silicate uptake ability not in the early stage, but rather in the later stage of cultivation with olivine addition (Fig. 2h). *T. pseudonana* benefited most from the addition of olivine, most likely due to its greater silicate demand compared to the other two phytoplankton species.

### 3.4. The potential effects of the trace metal released from olivine dissolution

$\text{Mg}^{2+}$  released from olivine dissolution may also contribute to the enhancement of olivine dissolution by phytoplankton growth.  $\text{Mg}^{2+}$ , the

second most abundant cation in cells (Romani, 2011), is an essential metal ion in the chlorophyll molecule and affects the growth of phytoplankton. Within a certain range, increasing the concentration of  $\text{Mg}^{2+}$  can increase the growth rate and biomass of phytoplankton (Ouyang et al., 2018; Xie et al., 2023). Metals like iron released from olivine dissolution required by phytoplankton can affect the growth of phytoplankton as well. Iron can act as a cofactor for enzymes that catalyze reactions involving the transfer of electrons such as photosynthesis, respiration, and the synthesis of essential organic molecules (Gao et al., 2021). Iron was found to stimulate phytoplankton's growth in iron-limited sea areas and induce phytoplankton blooms, known as iron fertilization (Boyd et al., 2007). It is reasonable to speculate that the iron released from olivine dissolution may stimulate the growth of phytoplankton. However, the rapid oxidation of Fe(II) to Fe(III) in seawater, followed by the formation of Fe(III)-Si-rich coatings, may prevent further dissolution of olivine (Saldi et al., 2013). It is thought that diatoms are able to absorb and utilize both Fe(II) and Fe(III) (Gao et al., 2021), theoretically diatoms may be able to help prevent the formation of Fe(III)-Si-rich coatings.

$\text{Mg}^\#$  ( $\text{Mg}/(\text{Mg} + \text{Fe})$ ) value based on Raman spectroscopy (Mouri and Enami, 2008) was lower on the surface of olivine without phytoplankton after 45 days of dissolution compared to the olivine with phytoplankton and pristine olivine (Table 1). Based on results derived from XPS, the pristine olivine had a higher Mg to Fe content ratio compared to the olivine dissolved in the presence of phytoplankton, while the lowest Mg to Fe content ratio was found on the olivine that dissolved in the absence of phytoplankton (Table S5). These results indicate a relatively higher Fe content on the olivine surface after 45 days of dissolution in the absence of phytoplankton compared to that on the olivine surface in the presence of phytoplankton. These findings are probably due to the precipitation of the Fe-containing phase on the olivine surface in the absence of phytoplankton, also corroborate with the possible absorption and utilization of Fe(III) by not only diatoms but also coccolithophores (Gao et al., 2021). Due to the low Fe content of the olivine we used, Eqs. (1)–(3) in Table 1 have limited precision, making the Mg content different from the Mg: Fe = 0.92:0.08 obtained from the compositional analysis, and no characteristic peaks of Fe-containing compounds were read from the Raman data, therefore the type of Fe compound and the valence of Fe could not be determined.

In a recent study, two silicifying diatoms, a calcifying coccolithophore, and three cyanobacteria showed both positive and neutral responses but no obvious toxic effects under elevated concentrations of olivine dissolution products using a synthetic olivine leachate (OL) based on olivine elemental composition. These findings suggest that phytoplanktons are likely to withstand the nickel and cobalt produced by olivine (Hutchins et al., 2023). Another recent study has shown that 11 marine phytoplankton species, especially *P. tricornutum*, have tolerance to very high nickel concentrations (e.g.  $50 \mu\text{mol L}^{-1}$ ) (Guo et al., 2022). If the olivine particles in our study were totally dissolved, which was not possible in any case, the Ni concentration would reach  $3.35 \mu\text{mol L}^{-1}$  based on the olivine composition analysis, which is still far

**Table 1**

The  $\text{Mg}^\#$  value was calculated based on the peaks of  $847\text{--}858 \text{ cm}^{-1}$  and  $815\text{--}825 \text{ cm}^{-1}$  in the Raman spectroscopy (Mouri and Enami, 2008).

$$\text{Mg}^\# = \left[ \frac{\text{Mg}}{\text{Mg} + \text{Fe}^{2+}} \right] (1)$$

$$\text{Mg}^\# = -0.17744 - 0.050049\omega + 0.0026479\omega^2 \quad (r^2 = 0.99) (2)$$

$$\omega = \kappa_1 - \kappa_2 (\text{cm}^{-1}) (3)$$

Group	$\kappa_1$ ( $\text{cm}^{-1}$ )	$\kappa_2$ ( $\text{cm}^{-1}$ )	$\omega$ ( $\text{cm}^{-1}$ )	$\text{Mg}^\#$
Olivine with <i>G. oceanica</i>	853.934	821.953	31.981	0.930
Olivine with <i>T. pseudonana</i>	855.098	823.131	31.967	0.928
Olivine with <i>P. tricornutum</i>	855.281	823.301	31.980	0.930
Olivine without phytoplankton	856.777	824.817	31.900	0.920
Pristine olivine	855.098	823.131	31.967	0.928

lower than the maximum tolerable concentration for 11 phytoplankton species as shown in Guo et al. (2022). Similarly, the concentration of Co was  $0.18 \mu\text{mol L}^{-1}$  if olivine particles were completely dissolved, which is lower than the safe cobalt concentration of  $0.31 \mu\text{mol L}^{-1}$  for three diatom species, as shown in a previous study (Karthikeyan et al., 2019). Therefore, the nickel and cobalt released from olivine dissolution likely did not have had negative effects on the phytoplankton's growth in our study. Not to be overlooked is the fact that olivine dissolution also releases the trace element chromium. The chemistry of this element is complex in the ocean, and the ecological effects of Cr(III) and Cr(VI) on phytoplankton are not uniform (Flipkens et al., 2021). Their possible toxicity to phytoplankton needs to be considered in the subsequent large-scale implementation of ocean alkalinity enhancement.

### 3.5. Co-culturing the highly silicified diatom with olivine particles enhanced stoichiometric olivine dissolution

One of the main barriers to olivine dissolution is nonstoichiometric dissolution, which results in the formation of silica-rich layers on the

surface of olivine at the nanometer scale and prevents further olivine dissolution (Béarat et al., 2006; Oelkers et al., 2018; Velbel, 1993). Pristine olivine particles were characterized by smooth surfaces, where the steps between adjacent terraces of the crystal facets could be visualized in the SEM image (Fig. 3a). The olivine surfaces in controls without phytoplankton remained relatively smooth (Fig. 3b). The surface of olivine after cultivation of *T. pseudonana* (Fig. 3c) was relatively rougher than those seen after growth of *P. tricornutum* (Fig. 3d) and *G. oceanica* (Fig. 3e). The apparent roughening in the former case is probably due to the utilization of the silicate constituents from olivine by *T. pseudonana*. Surface roughening was also revealed in the dissolving olivine in the presence of *P. tricornutum* for a different reason, as this led to the formation of mineral particles covered with fibrous organic components. It is very likely that these fibrous structures were extracellular polymeric substances (EPS) (Shirokova et al., 2012) secreted by *P. tricornutum*. The coverage of individual mineral particles with these polymeric components may explain the impedance of the continuous dissolution of olivine in the presence of *P. tricornutum*.

Based on the EDS finding, the atomic ratios of magnesium and silicon

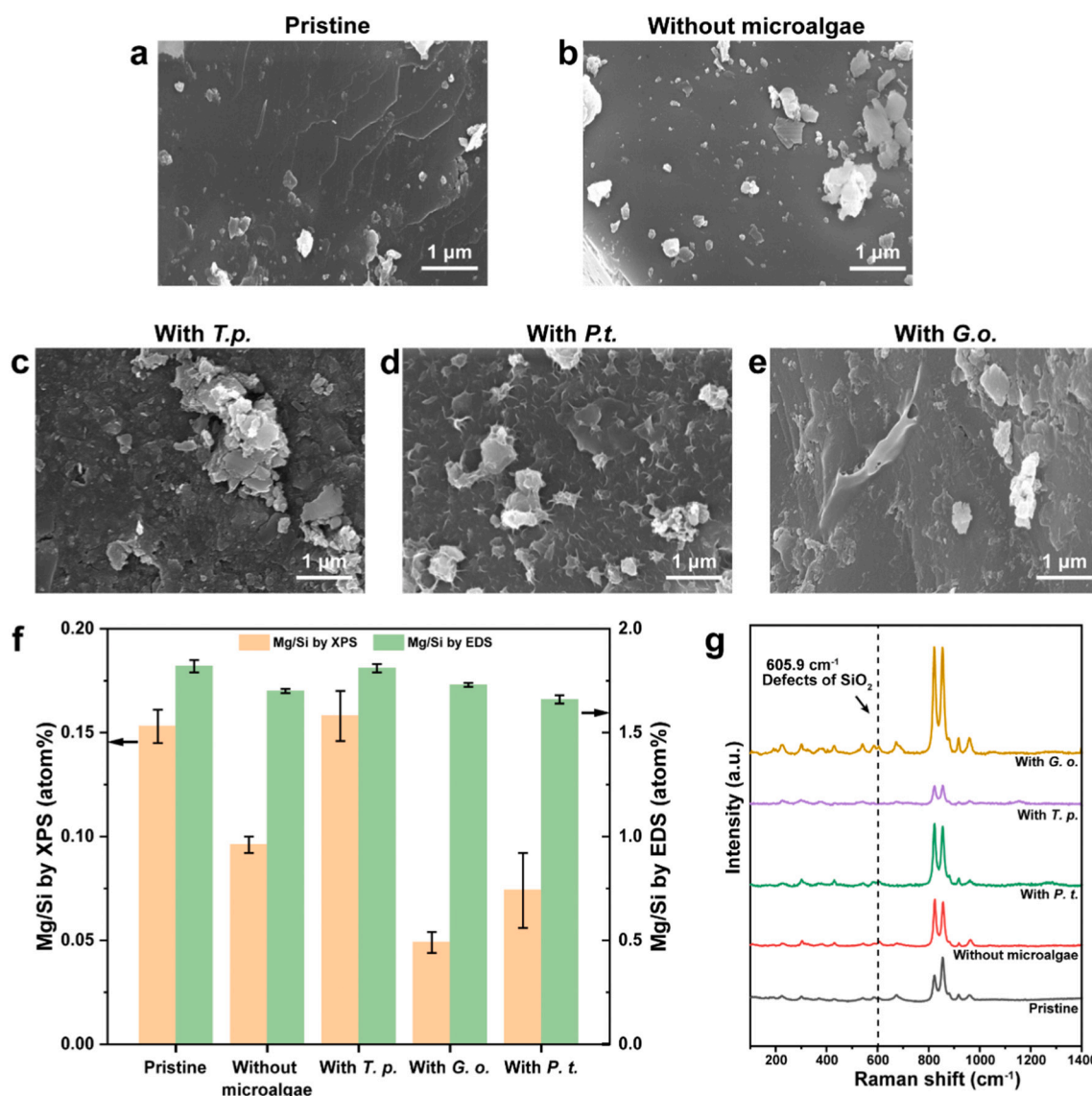


**Fig. 3.** Scanning Electron Microscopy (SEM) images show the microstructural characteristics of olivine surfaces in the absence of phytoplankton: initial (a) and after 45 days dissolution (b), and in the presence of phytoplankton: *T. pseudonana* (c), *P. tricornutum* (d) and *G. oceanica* (e). The values of Mg/Si of different olivine surfaces with X-ray photoelectron spectroscopy (XPS) and Energy dispersive spectroscopy (EDS) (f). Characterization of different olivine surfaces with Raman spectroscopy (g).

(Mg/Si) on the surface of olivine decreased after 45 days of dissolution without microalgae, which also occurred in *G. oceanica* or *P. tricorutum* induced olivine dissolution (Fig. 3f, Table S5). The lower Mg/Si value on the olivine surface after dissolution for 45 days was probably due to the formation and deposition of a silica-rich layer from the silicate released from olivine dissolution (Bates et al., 1974; Galeener and Mikkelsen, 1981). The Mg/Si on the surface of olivine in the presence of *T. pseudonana* was close to that found on the pristine olivine surface (Fig. 3f, Table S5). The XPS results also demonstrate that the Mg/Si ratio of the olivine dissolved in the presence of *T. pseudonana* was close to that of pristine olivine. In comparison, the Mg/Si ratios of the olivine dissolved in the presence of *G. oceanica* or *P. tricorutum* and that dissolved in the abiotic control condition were relatively low, when compared with the values mentioned above (Fig. 3f, Table S5). Based on results derived from both EDS and XPS, the Mg/Si value on the surface of olivine in the presence of *T. pseudonana* was comparable to that of pristine olivine, which demonstrates that *T. pseudonana* facilitated the stoichiometric dissolution of olivine in seawater.

A peak at  $605.9\text{ cm}^{-1}$  representing the amorphous  $\text{SiO}_2$  layer was detected by Raman spectroscopy on the surface of olivine in the absence of phytoplankton and in the presence of *P. tricorutum* and *G. oceanica* (Fig. 3g) (Bates et al., 1974; Galeener and Mikkelsen, 1981). This peak was not detected on the surface of pristine olivine or olivine in the presence of *T. pseudonana* (Fig. 3g). Surface protonation leads to the release of  $\text{Mg}^{2+}$  and meanwhile, promotes the condensed polymerization of the  $\text{SiO}_4^{2-}$  groups that evolves into a continuous silica nano-coating on dissolving olivine (Pokrovsky and Schott, 2000). We speculate that the formation of amorphous  $\text{SiO}_2$  was due to non-stoichiometric dissolution and the changes in olivine surface structure during dissolution. Taken together, our results suggest that olivine dissolution can be enhanced by diatoms, especially those with thick siliceous walls, by facilitating stoichiometric dissolution (Fig. 4).

#### 4. Conclusion and perspective

Our study demonstrated that the dissolution of olivine in seawater can promote the growth of phytoplankton, including diatoms and coccolithophores, with more pronounced positive effects on the highly silicified diatom. Our findings imply that diatoms may outcompete other phytoplankton, such as coccolithophores, with an increase in primary production, which is in line with previously predicted ecological consequences of spreading olivine particles in the ocean (Bach et al., 2019). On the other hand, highly silicified diatoms can promote the

stoichiometric dissolution of olivine, which may also enhance carbon sequestration. This study is the first to examine the interactions between marine phytoplankton and olivine dissolution in seawater and provides valuable insights into ocean-based CDR (Fig. 4).

Although our study demonstrated no negative effects of olivine dissolution on the phytoplankton strains we examined, the potential toxicity of olivine dissolution should be further explored. Future studies should focus on long-term experiments involving not only phytoplankton but also other marine organisms. Our findings indicate that the marine community composition may change if we use olivine to alkalinize the ocean, which may have a significant impact on the marine ecosystem and biogeochemical cycling. In the future, the impacts of olivine dissolution in the ocean should be evaluated by lab experiments, mesocosm experiments, and ocean geoengineering scheme field tests. Additionally, the processes for obtaining small-sized olivine, such as mineral crushing and transportation, may cause particle contamination and other environmental problems that may limit its applicability. Therefore, the large-scale application of marine alkalinity enhancement using olivine requires an assessment of its carbon balance and potential negative environmental effects using methods such as Life Cycle Impact Assessment (LCA) (Foteinis et al., 2023).

#### CRedit authorship contribution statement

**Canru Li:** Performed the experiments, Drafted the manuscript, Data curation, Developed data visualizations, Review and Editing.

**Xiangdong Liu:** Performed the experiments, Drafted the manuscript, Data curation.

**Yan Li:** Performed the experiments, Revised the manuscript.

**Yuan Jiang:** Contributed to the conception of the study, Drafted the manuscript.

**Xianghui Guo:** Contributed to the conception of the study, Revised the manuscript.

**David A. Hutchins:** Revised the manuscript.

**Jian Ma:** Revised the manuscript.

**Xin Lin:** Contributed to the conception of the study, Supervised the study, Drafted the manuscript, Reviewing and editing.

**Minhan Dai:** Contributed to the conception of the study.

#### Declaration of competing interest

The authors declare that they have no known competing financial interests or personal relationships that could have appeared to influence

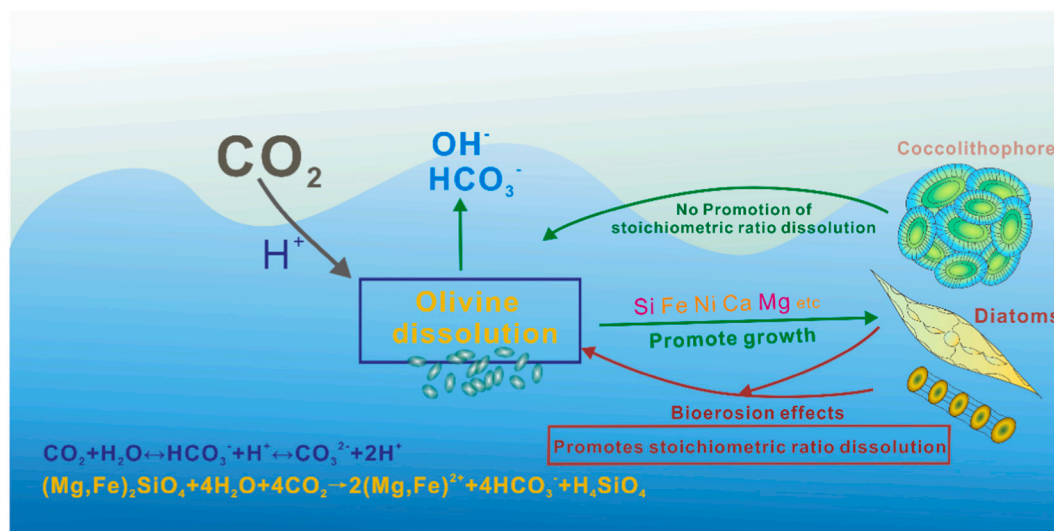


**Fig. 4.** Diagram of the mechanism of interaction between diatoms and olivine dissolution. Diatoms use Si to facilitate olivine stoichiometric ratio dissolution, bringing bioerosion to the olivine, while dissolved materials from the olivine contribute to phytoplankton growth.

the work reported in this paper.

## Data availability

Data will be made available on request.

## Acknowledgement

This work was supported by State key Laboratory of Marine environmental Science (Xiamen University) (MEL) Internal Program No. MELR12202 and Fujian Provincial Research Institutes of Basic Research and Public Service Special Operations (2021R1007007).

## Appendix A. Supplementary data

Supplementary data to this article can be found online at <https://doi.org/10.1016/j.scitotenv.2023.168571>.

## References

- Armbrust, E.V., 2009. The life of diatoms in the world's oceans. *Nature* 459, 185–192.
- Bach, L.T., Gill, S.J., Rickaby, R.E.M., Gore, S.J., Renforth, P., 2019. CO<sub>2</sub> removal with enhanced weathering and ocean alkalinity enhancement: potential risks and co-benefits for marine pelagic ecosystems. *Front. Clim* 1, 7.
- Bates, J., Hendricks, R., Shaffer, L., 1974. Neutron irradiation effects and structure of noncrystalline SiO<sub>2</sub>. *J. Chem. Phys.* 61, 4163–4176.
- Béarat, H., McKelvy, M.J., Chizmeshya, A.V.G., Gormley, D., Nunez, R., Carpenter, R.W., et al., 2006. Carbon sequestration via aqueous olivine mineral carbonation: role of passivating layer formation. *Environ. Sci. Technol.* 40, 4802–4808.
- Boyd, P.W., Jickells, T., Law, C., Blain, S., Boyle, E., Buesseler, K., et al., 2007. Mesoscale iron enrichment experiments 1993–2005: synthesis and future directions. *Science* 315, 612–617.
- Colman, B., Huertas, I.E., Bhatti, S., Dason, J.S., 2002. The diversity of inorganic carbon acquisition mechanisms in eukaryotic microalgae. *Funct. Plant Biol.* 29, 261–270.
- Flipkens, G., Blust, R., Town, R.M., 2021. Deriving nickel (Ni (II)) and chromium (Cr (III)) based environmentally safe olivine guidelines for coastal enhanced silicate weathering. *Environ. Sci. Technol.* 55, 12362–12371.
- Foteinis, S., Campbell, J., Renforth, P., 2023. Life cycle assessment of coastal enhanced weathering for carbon dioxide removal from air. *Environ. Sci. Technol.* 57.
- Friedlingstein, P., Jones, M.W., O'Sullivan, M., Andrew, R.M., Bakker, D.C., Hauck, J., et al., 2022. Global carbon budget 2021. *Earth Syst. Sci. Data* 14, 1917–2005.
- Galeener, F.L., Mikkelsen, J.C., 1981. Raman studies of the thermal oxide of silicon. *Solid State Commun.* 37, 719–723.
- Gao, X., Bowler, C., Kazamia, E., 2021. Iron metabolism strategies in diatoms. *J. Exp. Bot.* 72, 2165–2180.
- Gardner, R.D., Cooksey, K.E., Mus, F., Macur, R., Moll, K., Eustance, E., et al., 2012. Use of sodium bicarbonate to stimulate triacylglycerol accumulation in the chlorophyte *Scenedesmus* sp. and the diatom *Phaeodactylum tricornutum*. *J. Appl. Phycol.* 24, 1311–1320.
- Genty, B., Briantais, J.-M., Baker, N.R., 1989. The relationship between the quantum yield of photosynthetic electron transport and quenching of chlorophyll fluorescence. *BBA-Gen. Subjects* 990, 87–92.
- Gerrits, R., Pokharel, R., Breitenbach, R., Radnik, J., Feldmann, I., Schuessler, J.A., et al., 2020. How the rock-inhabiting fungus *G. petricola* A95 enhances olivine dissolution through attachment. *Geochim. Cosmochim. Acta* 282, 76–97.
- Giordano, M., Beardall, J., Raven, J.A., 2005. CO<sub>2</sub> concentrating mechanisms in algae: mechanisms, environmental modulation, and evolution. *Annu. Rev. Plant Biol.* 56, 99–131.
- Goll, D.S., Ciais, P., Amann, T., Buermann, W., Chang, J., Eker, S., et al., 2021. Potential CO<sub>2</sub> removal from enhanced weathering by ecosystem responses to powdered rock. *Nat. Geosci.* 14, 545–549.
- González, M.F., Ilyina, T., 2016. Impacts of artificial ocean alkalization on the carbon cycle and climate in Earth system simulations. *Geophys. Res. Lett.* 43, 6493–6502.
- Guo, J.A., Strzpek, R., Willis, A., Ferderer, A., Bach, L.T., 2022. Investigating the effect of nickel concentration on phytoplankton growth to assess potential side-effects of ocean alkalinity enhancement. *Biogeosciences* 19, 3683–3697.
- Hangx, S.J.T., Spiers, C.J., 2009. Coastal spreading of olivine to control atmospheric CO<sub>2</sub> concentrations: a critical analysis of viability. *Int. J. Greenhouse Gas Control* 3, 757–767.
- Hilaire, J., Minx, J.C., Callaghan, M.W., Edmonds, J., Luderer, G., Nemet, G.F., et al., 2019. Negative emissions and international climate goals—learning from and about mitigation scenarios. *Clim. Chang.* 157, 189–219.
- Huang, T., Hu, F., Pan, Y., Li, C., Hu, H., 2023. Pyruvate orthophosphate dikinase is required for the acclimation to high bicarbonate concentrations in *Phaeodactylum tricornutum*. *Algal Res.* 72, 103131.
- Hutchins, D.A., Fu, F.-X., Yang, S.-C., John, S.G., Romaniello, S.J., Andrews, M.G., et al., 2023. Responses of globally important phytoplankton species to olivine dissolution products and implications for carbon dioxide removal via ocean alkalinity enhancement. *bioRxiv* (2023.04.08.536121).
- IPCC, 2022. Impacts of 1.5°C global warming on natural and human systems. In: Intergovernmental Panel on Climate Change, editor. *Global Warming of 1.5°C: IPCC Special Report on Impacts of Global Warming of 1.5°C above Pre-industrial Levels in Context of Strengthening Response to Climate Change, Sustainable Development, and Efforts to Eradicate Poverty*. Cambridge University Press, Cambridge, pp. 175–312.
- Jongmans, A.G., van Breemen, N., Lundström, U., van Hees, P.A.W., Finlay, R.D., Srinivasan, M., et al., 1997. Rock-eating fungi. *Nature* 389, 682–683.
- Karthikeyan, P., Marigoudar, S.R., Nagarjuna, A., Sharma, K.V., 2019. Toxicity assessment of cobalt and selenium on marine diatoms and copepods. *Environ. Chem. Ecotoxicol.* 1, 36–42.
- Kheshgi, H.S., 1995. Sequestering atmospheric carbon dioxide by increasing ocean alkalinity. *Energy* 20, 915–922.
- Montserrat, F., Renforth, P., Hartmann, J., Leermakers, M., Knops, P., Meysman, F.J.R., 2017. Olivine dissolution in seawater: implications for CO<sub>2</sub> sequestration through enhanced weathering in coastal environments. *Environ. Sci. Technol.* 51, 3960–3972.
- Mouri, T., Enami, M., 2008. Raman spectroscopic study of olivine-group minerals. *J. Mineral. Petrol. Sci.* 103, 100–104.
- National Academies of Sciences E, Medicine, 2021. *A Research Strategy for Ocean-based Carbon Dioxide Removal and Sequestration*.
- Oelkers, E.H., Benning, L.G., Lutz, S., Mavromatis, V., Pearce, C.R., Plümper, O., 2015. The efficient long-term inhibition of forsterite dissolution by common soil bacteria and fungi at Earth surface conditions. *Geochim. Cosmochim. Acta* 168, 222–235.
- Oelkers, E.H., Declercq, J., Saldi, G.D., Gislason, S.R., Schott, J., 2018. Olivine dissolution rates: a critical review. *Chem. Geol.* 500, 1–19.
- Ouyang, Z., Chen, R., Liu, Q., He, L., Cai, W.-J., Yin, K., 2018. Biological regulation of carbonate chemistry during diatom growth under different concentrations of Ca<sup>2+</sup> and Mg<sup>2+</sup>. *Mar. Chem.* 203, 38–48.
- Pokrovsky, O.S., Schott, J., 2000. Forsterite surface composition in aqueous solutions: a combined potentiometric, electrokinetic, and spectroscopic approach. *Geochim. Cosmochim. Acta* 64, 3299–3312.
- Pozo, C., Galán-Martín, Á., Reiner, D.M., Mac Dowell, N., Guillén-Gosálbez, G., 2020. Equity in allocating carbon dioxide removal quotas. *Nat. Clim. Chang.* 10, 640–646.
- Prigobbe, V., Hänchen, M., Costa, G., Baciocchi, R., Mazzotti, M., 2009. Analysis of the effect of temperature, pH, CO<sub>2</sub> pressure and salinity on the olivine dissolution kinetics. *Energy Procedia* 1, 4881–4884.
- Rigopoulos, I., Harrison, A.L., Delimitis, A., Ioannou, I., Efstathiou, A.M., Kyratsi, T., et al., 2018. Carbon sequestration via enhanced weathering of peridotites and basalts in seawater. *Appl. Geochem.* 91, 197–207.
- Rockström, J., Gaffney, O., Rogelj, J., Meinshausen, M., Nakicenovic, N., Schellnhuber, H.J., 2017. A roadmap for rapid decarbonization. *Science* 355, 1269–1271.
- Rogelj, J., Popp, A., Calvin, K.V., Luderer, G., Emmerling, J., Gernaat, D., et al., 2018. Scenarios towards limiting global mean temperature increase below 1.5 °C. *Nat. Clim. Chang.* 8, 325–332.
- Romani, A.M.P., 2011. Cellular magnesium homeostasis. *Arch. Biochem. Biophys.* 512, 1–23.
- Saldi, G.D., Daval, D., Morvan, G., Knauss, K.G., 2013. The role of Fe and redox conditions in olivine carbonation rates: an experimental study of the rate limiting reactions at 90 and 150 °C in open and closed systems. *Geochim. Cosmochim. Acta* 118, 157–183.
- Schilling, R.D., Boer, Pld, 2011. Rolling stones; fast weathering of olivine in shallow seas for cost-effective CO<sub>2</sub> capture and mitigation of global warming and ocean acidification. *Earth Syst. Dyn. Discuss.* 2, 551–568.
- Seiffert, F., Bandow, N., Bouchez, J., von Blanckenburg, F., Gorbushina, A.A., 2014. Microbial colonization of bare rocks: laboratory biofilm enhances mineral weathering. *Procedia Earth Planet. Sci.* 10, 123–129.
- Shirokova, L.S., Bénézet, P., Pokrovsky, O.S., Gerard, E., Ménez, B., Alfredsson, H., 2012. Effect of the heterotrophic bacterium *Pseudomonas* reactans on olivine dissolution kinetics and implications for CO<sub>2</sub> storage in basalts. *Geochim. Cosmochim. Acta* 80, 30–50.
- Strickland, J.D.H., Parsons, T.R., 1972. *A practical handbook of seawater analysis*. Fish. Res. Board Canada 310.
- Tsuji, Y., Mahardika, A., Matsuda, Y., 2017. Evolutionarily distinct strategies for the acquisition of inorganic carbon from seawater in marine diatoms. *J. Exp. Bot.* 68, 3949–3958.
- Velbel, M.A., 1993. Formation of protective surface layers during silicate-mineral weathering under well-leached, oxidizing conditions. *Am. Mineral.* 78, 405–414.
- Vicca, S., Goll, D.S., Hagens, M., Hartmann, J., Janssens, I.A., Neubeck, A., et al., 2022. Is the climate change mitigation effect of enhanced silicate weathering governed by biological processes? *Glob. Chang. Biol.* 28, 711–726.
- West, A.J., Galy, A., Bickle, M., 2005. Tectonic and climatic controls on silicate weathering. *Earth Planet. Sci. Lett.* 235, 211–228.
- White, D., Pagarette, A., Rooks, P., Ali, S., 2013. The effect of sodium bicarbonate supplementation on growth and biochemical composition of marine microalgae cultures. *J. Appl. Phycol.* 25, 153–165.
- Xie, T., Wu, Y., 2014. The role of microalgae and their carbonic anhydrase on the biological dissolution of limestone. *Environ. Earth Sci.* 71, 5231–5239.
- Xie, T., Zhao, L., Wu, Y., 2023. Peridotite dissolution in the presence of green microalgae: implications for a geoengineering strategy of CO<sub>2</sub> sequestration. *J. Asian Earth Sci.* 241, 105486.
- Zerveas, S., Mente, M.S., Tsakiri, D., Kotzabasis, K., 2021. Microalgal photosynthesis induces alkalization of aquatic environment as a result of H<sup>+</sup> uptake independently from CO<sub>2</sub> concentration – new perspectives for environmental applications. *J. Environ. Manag.* 289, 112546.